

Electronic Supporting Information

Experimental and theoretical investigations of magnetic exchange pathways in structurally diverse iron(III) Schiff-base complexes

Radovan Herchel, Ivan Nemec, Marek Machata, Zdeněk Trávníček *

Regional Centre of Advanced Technologies and Materials, Department of Inorganic Chemistry,
Faculty of Science, Palacký University, 17. listopadu 12, CZ-771 46 Olomouc, Czech Republic.

Table S1. The B3LYP/def2-TZVP calculated net Mulliken spin densities, the $\langle S^2 \rangle$ values and relative energies of broken-symmetry spin states for dimeric fragments of $K[FeL_2] \cdot H_2O$ (**1**) based on the experimental (X-ray) geometry.

{[FeL ₂]⋯K(H ₂ O)⋯[FeL ₂]} ⁻ of 1			{[K(H ₂ O)FeL ₂]⋯[FeL ₂ K(H ₂ O)]} of 1		
	HS	BS		HS	BS
$\rho(Fe1)$	4.22	-4.22	$\rho(Fe1)$	4.22	-4.22
$\rho(N1)$	0.07	-0.07	$\rho(N1)$	0.06	-0.06
$\rho(N2A)$	0.06	-0.06	$\rho(N2A)$	0.08	-0.07
$\rho(O4)$	0.14	-0.14	$\rho(O4)$	0.11	-0.11
$\rho(O1)$	0.13	-0.13	$\rho(O1)$	0.12	-0.12
$\rho(O2)$	0.12	-0.12	$\rho(O2)$	0.12	-0.12
$\rho(O3)$	0.12	-0.12	$\rho(O3)$	0.16	-0.16
$\rho(K1)$	0.005	-0.0006			
$\rho(O1')$	0.13	0.13	$\rho(O1')$	0.12	0.12
$\rho(O3')$	0.11	0.11	$\rho(O3')$	0.16	0.16
$\rho(O2')$	0.13	0.13	$\rho(O2')$	0.12	0.12
$\rho(O4')$	0.15	0.15	$\rho(O4')$	0.11	0.11
$\rho(N2A')$	0.06	0.06	$\rho(N2A')$	0.08	0.07
$\rho(N1')$	0.06	0.06	$\rho(N1')$	0.06	0.06
$\rho(Fe1')$	4.21	4.21	$\rho(Fe1')$	4.22	4.22
$\langle S^2 \rangle$	30.02	5.02	$\langle S^2 \rangle$	30.02	5.02
$E_{BS} - E_{HS}$	-0.782 cm ⁻¹		$E_{BS} - E_{HS}$	-2.913 cm ⁻¹	

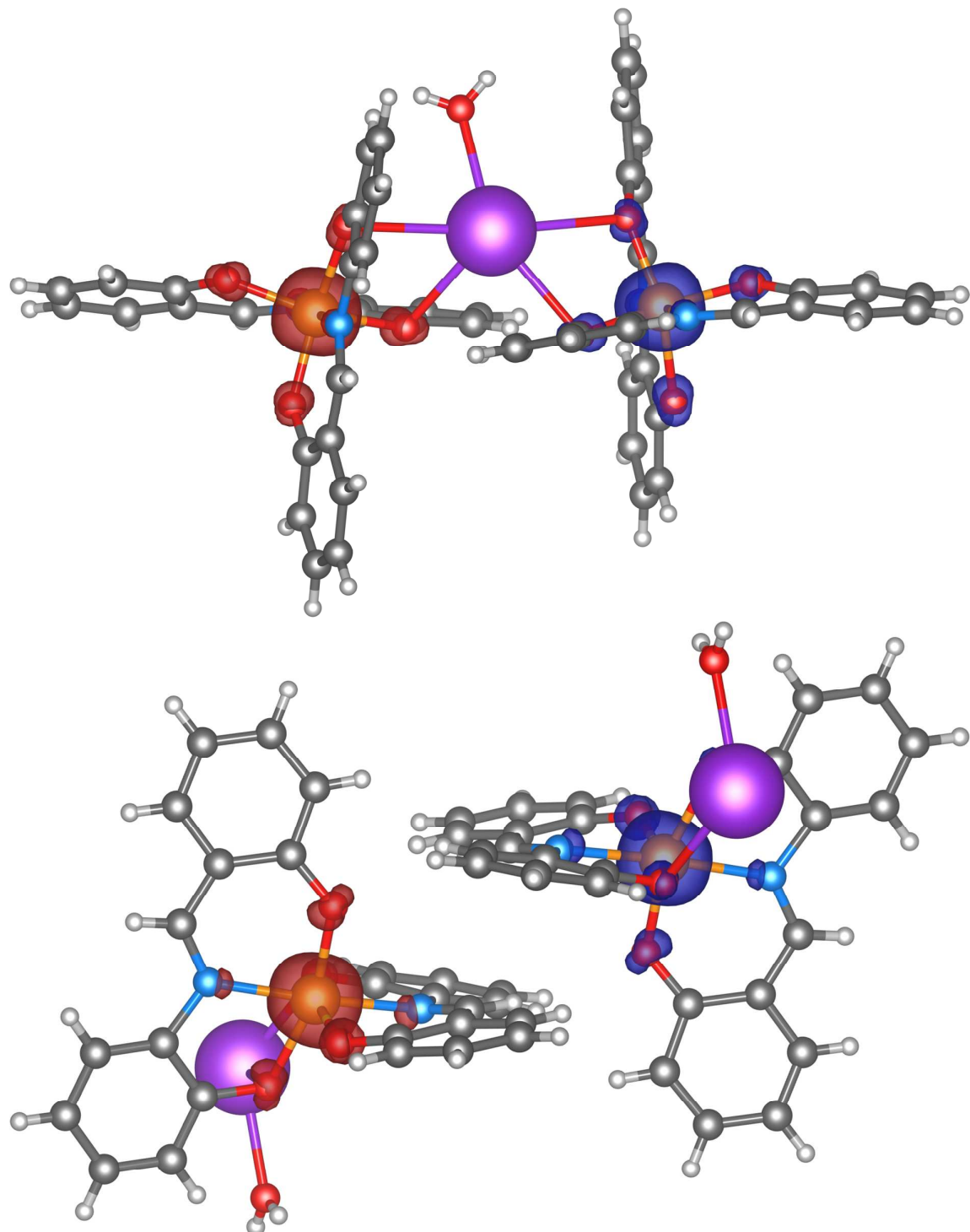


Fig. S1 The calculated spin density distribution for broken-symmetry spin state using B3LYP for the $\{[\text{FeL}_2] \cdots \text{K}(\text{H}_2\text{O}) \cdots [\text{FeL}_2]\}^-$ unit of **1** (top) and for $\{\text{[K}(\text{H}_2\text{O})\text{FeL}_2] \cdots [\text{FeL}_2\text{K}(\text{H}_2\text{O})]\}$ unit of **1** (bottom). Positive and negative spin densities are represented by dark blue and dark red surfaces, respectively. The isodensity surfaces are plotted with cutoff values of $0.02 \text{ } ea_0^{-3}$.

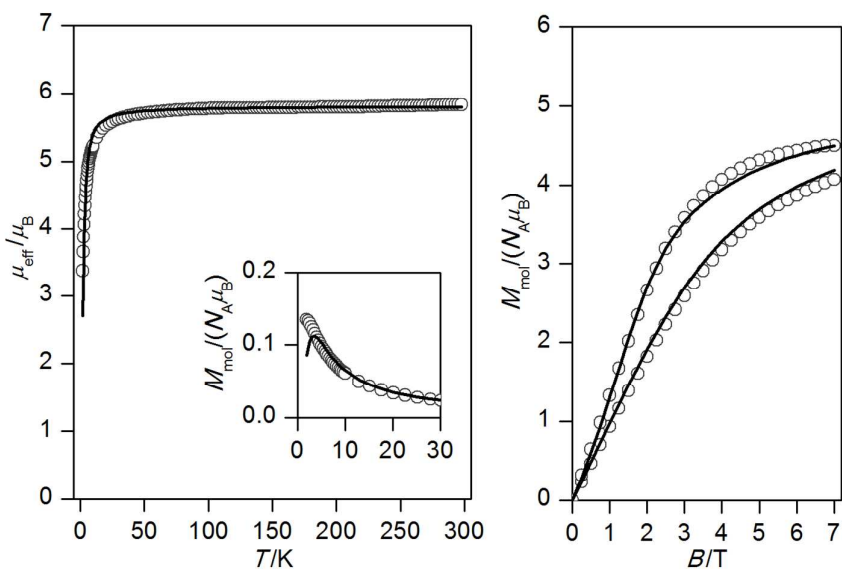


Fig. S2 The magnetic data for complex **1**. Left: the temperature dependence of the effective magnetic moment and molar magnetization measured at $B = 0.1 \text{ T}$. Right: the isothermal magnetizations measured at $T = 2.0$ and 5 K . Empty circles – experimental data, full lines – calculated data using the Eq. (3) and $J = -0.29(3) \text{ cm}^{-1}$, $D = -1.2(2) \text{ cm}^{-1}$ and $g = 1.964(7)$. The data are scaled per one iron(III) centre.

Table S2. The B3LYP/def2-TZVP calculated net Mulliken spin densities, the $\langle S^2 \rangle$ values and relative energies of broken-symmetry spin states for dimeric fragment of $\text{Pr}_3\text{NH}[\text{FeL}_2]$ (**2**) based on the experimental (X-ray) geometry.

{ $\text{Pr}_3\text{NH}[\text{FeL}_2] \cdots [\text{FeL}_2]\text{Pr}_3\text{NH}$ } of 2		
	HS	BS
$\rho(\text{Fe1})$	4.22	-4.22
$\rho(\text{O1})$	0.14	-0.14
$\rho(\text{N1A})$	0.07	-0.07
$\rho(\text{O2})$	0.11	-0.11
$\rho(\text{O3})$	0.15	-0.15
$\rho(\text{N2A})$	0.06	-0.06
$\rho(\text{O4})$	0.10	-0.10
$\rho(\text{O4}')$	0.10	0.10
$\rho(\text{N2A}')$	0.06	0.06
$\rho(\text{O3}')$	0.15	0.15
$\rho(\text{O2})$	0.11	0.11
$\rho(\text{N1A}')$	0.07	0.07
$\rho(\text{O1}')$	0.14	0.14
$\rho(\text{Fe1}')$	4.22	4.22
$\langle S^2 \rangle$	30.02	5.02
$E_{\text{BS}} - E_{\text{HS}}$	-0.331 cm^{-1}	

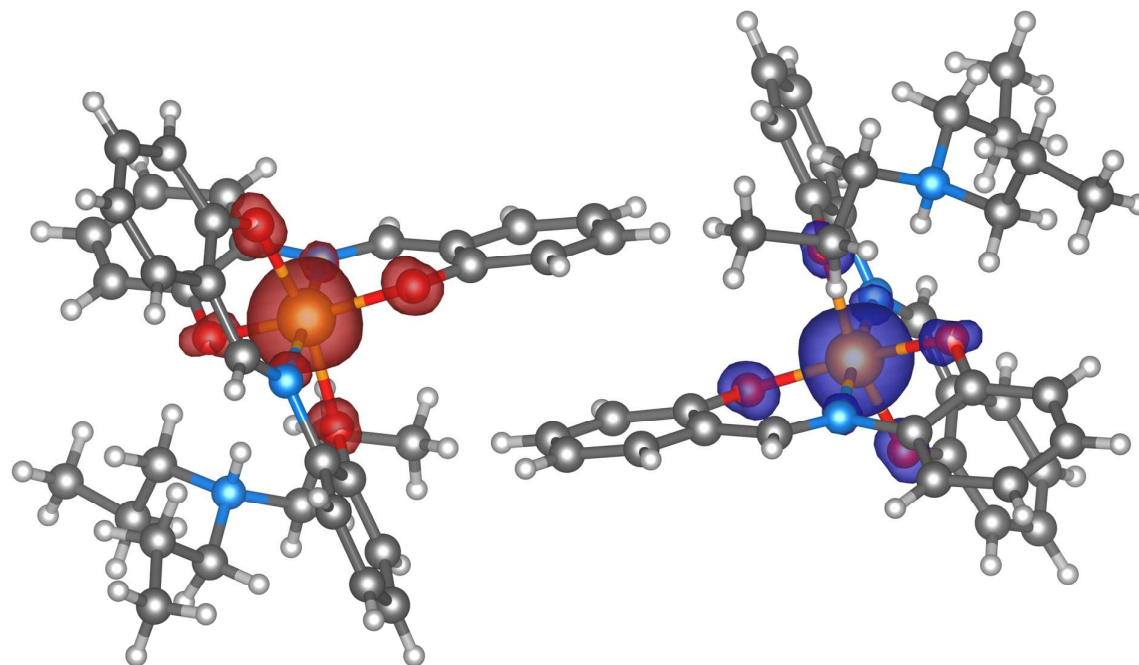


Fig. S3 The calculated spin density distribution for broken-symmetry spin state using B3LYP for the $\{\text{Pr}_3\text{NH}[\text{FeL}_2] \cdots [\text{FeL}_2]\text{Pr}_3\text{NH}\}$ unit of **2**. Positive and negative spin densities are represented by dark blue and dark red surfaces, respectively. The isodensity surfaces are plotted with cutoff values of $0.02 \text{ e } a_0^{-3}$.

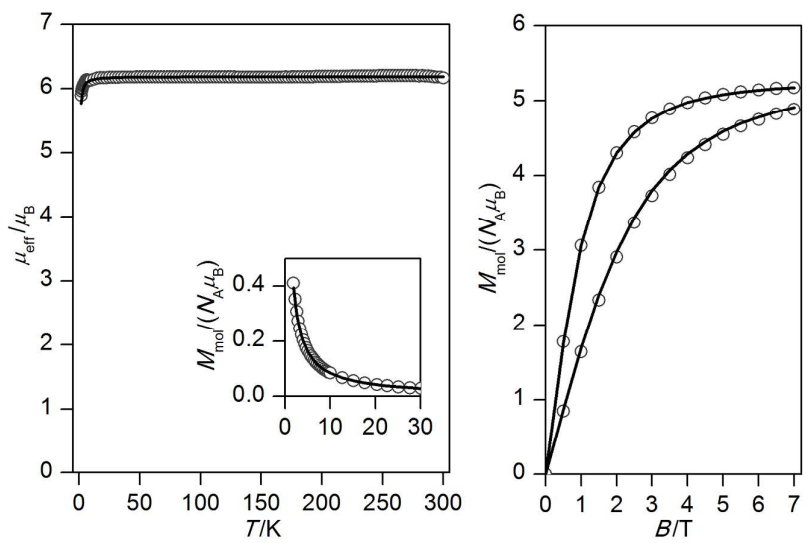


Fig. S4 The magnetic data for complex $(\text{Pr}_3\text{NH})[\text{FeL}_2]\cdot\text{H}_2\text{O}$ (**2**). Left: The temperature dependence of the effective magnetic moment and molar magnetization measured at $B = 0.1$ T. Right: The isothermal magnetizations measured at $T = 2.0$ and 4.6 K. Empty circles – experimental data, full lines – calculated data using the Eq. (4) and $J = -0.038(5)$ cm $^{-1}$, $D = +0.53(8)$ cm $^{-1}$ and $g = 2.091(2)$. The data are scaled per one iron(III) centre.

Table S3. The B3LYP/def2-TZVP calculated net Mulliken spin densities, the $\langle S^2 \rangle$ values and relative energies of broken-symmetry spin states for dimeric fragment of $[\text{FeL}(\text{bpyO}_2)(\text{CH}_3\text{OH})][\text{FeL}_2]$ (**3**) based on the experimental (X-ray) geometry.

	HS	BS
$\rho(\text{Fe1})$	4.21	4.21
$\rho(\text{N1})$	0.07	0.07
$\rho(\text{N2})$	0.07	0.07
$\rho(\text{O1})$	0.15	0.15
$\rho(\text{O2})$	0.08	0.07
$\rho(\text{O3})$	0.14	0.14
$\rho(\text{O4})$	0.13	0.13
$\rho(\text{H9B})$	0.002	-0.002
$\rho(\text{O9})$	0.06	-0.06
$\rho(\text{O8})$	0.07	0.06
$\rho(\text{O7})$	0.05	-0.05
$\rho(\text{O6})$	0.18	-0.18
$\rho(\text{O5})$	0.15	-0.15
$\rho(\text{N3})$	0.07	-0.07
$\rho(\text{Fe2})$	4.20	-4.20
$\langle S^2 \rangle$	30.02	5.02
$E_{\text{BS}} - E_{\text{HS}}$	-7.990 cm^{-1}	

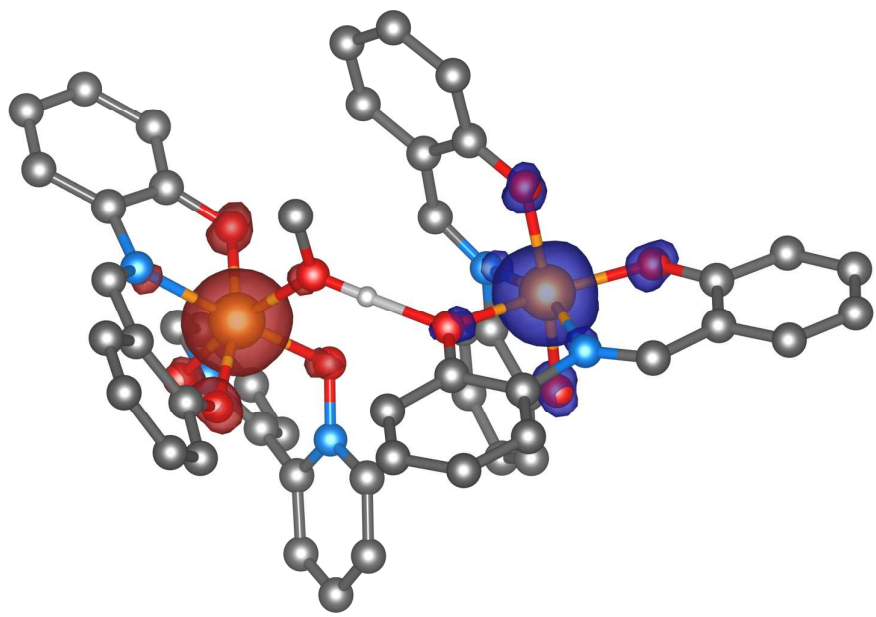


Fig. S5 The calculated spin density distribution for broken-symmetry spin state using B3LYP for the $\{[\text{FeL}(\text{bpyO}_2)(\text{CH}_3\text{OH})] \cdots [\text{FeL}_2]\cdot\text{CH}_3\text{OH}\}$ unit of **3**. Positive and negative spin densities are represented by dark blue and darkred surfaces, respectively. The isodensity surfaces are plotted with cutoff values of $0.02 \text{ } e\text{a}_0^{-3}$. Only hydrogen atoms involved in hydrogen bonding is shown.

Table S4. The B3LYP/def2-TZVP calculated net Mulliken spin densities, the $\langle S^2 \rangle$ values and relative energies of broken-symmetry spin states for dimeric fragment of $[\text{Fe}_2\text{L}_3(\text{CH}_3\text{OH})] \cdot 2\text{CH}_3\text{OH} \cdot \text{H}_2\text{O}$ (**4**) based on the experimental (X-ray) geometry.

{ $[\text{Fe}_2\text{L}_3(\text{CH}_3\text{OH})]$ } of 4		
	HS	BS
$\rho(\text{Fe1})$	4.22	-4.21
$\rho(\text{N1A})$	0.07	-0.07
$\rho(\text{O1})$	0.19	-0.19
$\rho(\text{O2})$	0.15	-0.15
$\rho(\text{O3})$	0.03	-0.03
$\rho(\text{O4})$	0.15	0.01
$\rho(\text{O5})$	0.15	-0.02
$\rho(\text{O6})$	0.17	0.17
$\rho(\text{O7})$	0.18	0.18
$\rho(\text{N3})$	0.08	0.08
$\rho(\text{N2})$	0.07	0.06
$\rho(\text{Fe2})$	4.20	4.19
$\langle S^2 \rangle$	30.02	4.99
$E_{\text{BS}} - E_{\text{HS}}$	-206.991 cm ⁻¹	

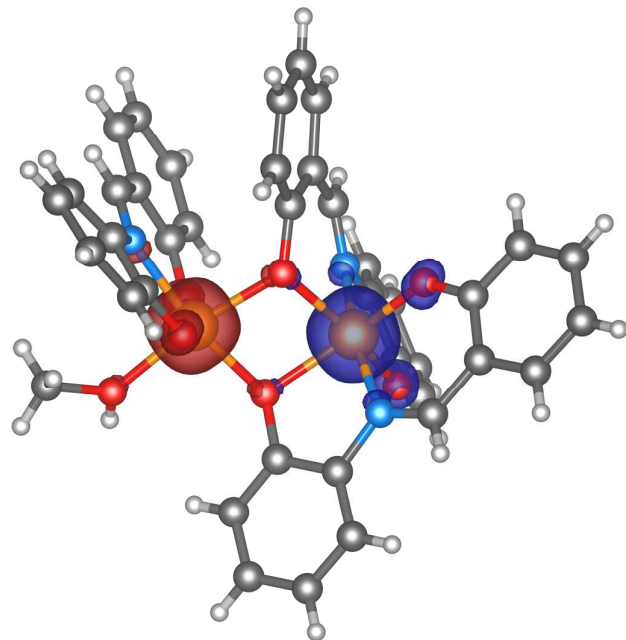


Fig. S6 The calculated spin density distribution high spin state and broken-symmetry state using B3LYP for the $[\text{Fe}_2\text{L}_3(\text{CH}_3\text{OH})]$ unit of **4**. Positive and negative spin densities are represented by dark blue and green surfaces, respectively. The isodensity surfaces are plotted with cutoff values of $0.02 \text{ } e\text{a}_0^{-3}$.

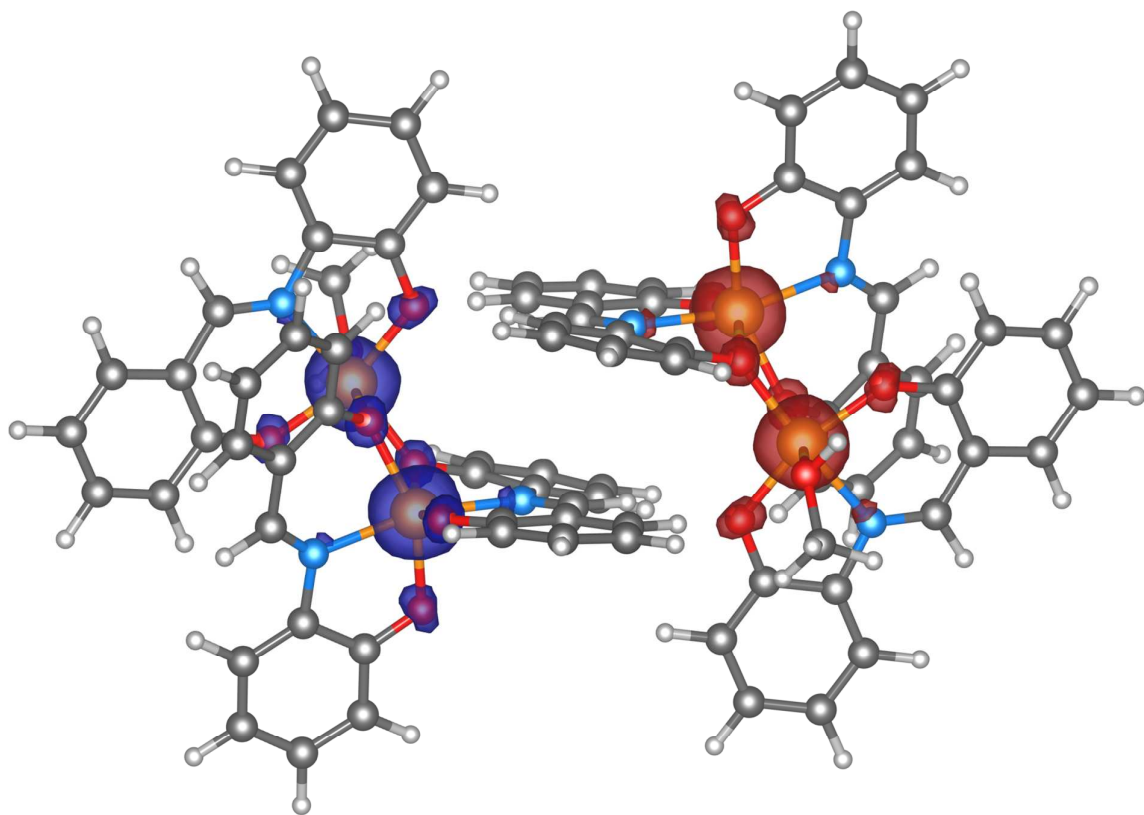


Fig. S7 The calculated spin density distribution for broken-symmetry spin state BS12 using B3LYP for the $\{[\text{Fe}_2\text{L}_3(\text{CH}_3\text{OH})]\}_2$ unit of **4**. Positive and negative spin densities are represented by dark blue and dark red surfaces, respectively. The isodensity surfaces are plotted with cutoff values of $0.02 \text{ } e\text{a}_0^{-3}$.